Civil Engineering
UNIVERSITY OF TORONTO

Numerical Simulation of Rock Fracturing under Laboratory True-Triaxial Stress Conditions

M. G. (Sherveen) Tabari, J. Hazzard, and R.P. Young

http://civil.engineering.utoronto.ca/staff/professors/paul-young/ Email: sherveen.m.g.tabari@alum.utoronto.ca LinkedIn: sherveentabari University of Toronto, Mining Building, Toronto, Ontario, Canada

European Geosciences Union General Assembly 2016
Vienna | Austria | 17–22 April 2016
EGU.eu

EGU2016-9221
April 20, 2016. Poster Number: **X2.97**.
Session Title: EMRP1.4/SM2.5/TS1.6, Earthquakes: from slow to fast, from the field to the laboratory.

Introduction

A True-triaxial test (TTT) also known as polyaxial test was carried out on 80 mm-side cubic saturated Fontainebleau sandstone under fixed σ_2=35 (Mpa) and σ_3=5 (Mpa) to elevate our knowledge about the role of the intermediate principal stress on deformation, fracturing and failure patterns of the rock using acoustic emission (AE) monitoring. The induced AE activities were studied by location of the AE events and mapping them on the captured features in the post-mortem CT scan images of the failed sample. The time-lapse monitoring of the velocity structure and AE activity in the sample portrayed a deformational path which led to propagation of fractures and formation of failure patterns in the rock. Having these experimental results, we aimed at running a numerical model of our true-triaxial testing system using an Itasca software based on three-dimensional explicit finite-difference method called FLAC3D. The loads were applied at the end of each platen while the steel platens transferred the stress to the surface of the cubic specimen. In order to simulate the failure, the Mohr-Columb failure criterion was implemented in all the spatial elements of the rock sample model. During the experiment, pseudo-boundary surfaces were formed along the minimum and intermediate principal stress axes in the rock due to non-uniform distribution of stress as a result of geometrical constraints including the corner effects and friction on the platen-rock surfaces. Both the real AE data as well as the numerical simulation verified that coalescence of micro-cracks mainly occurred around these pseudo-boundaries with highest stress gradients as well as highest velocity gradients in the rock specimen and formed curvi-planar fractures. The rock specimen strength and brittleness in the macro-scale was also obtained from the stress-strain curve which was consistent with the experimental laboratory measurements. Eventually, the failure of the rock specimen was simulated at the final stages of the experiment at higher effective stresses where an M-shaped form of through-going conjugate fractures was developed and their spatial orientations and angles were measured under various polyaxial loading conditions. This study enhances our understanding about the initiation and propagation of fractures under true-triaxial stress states.

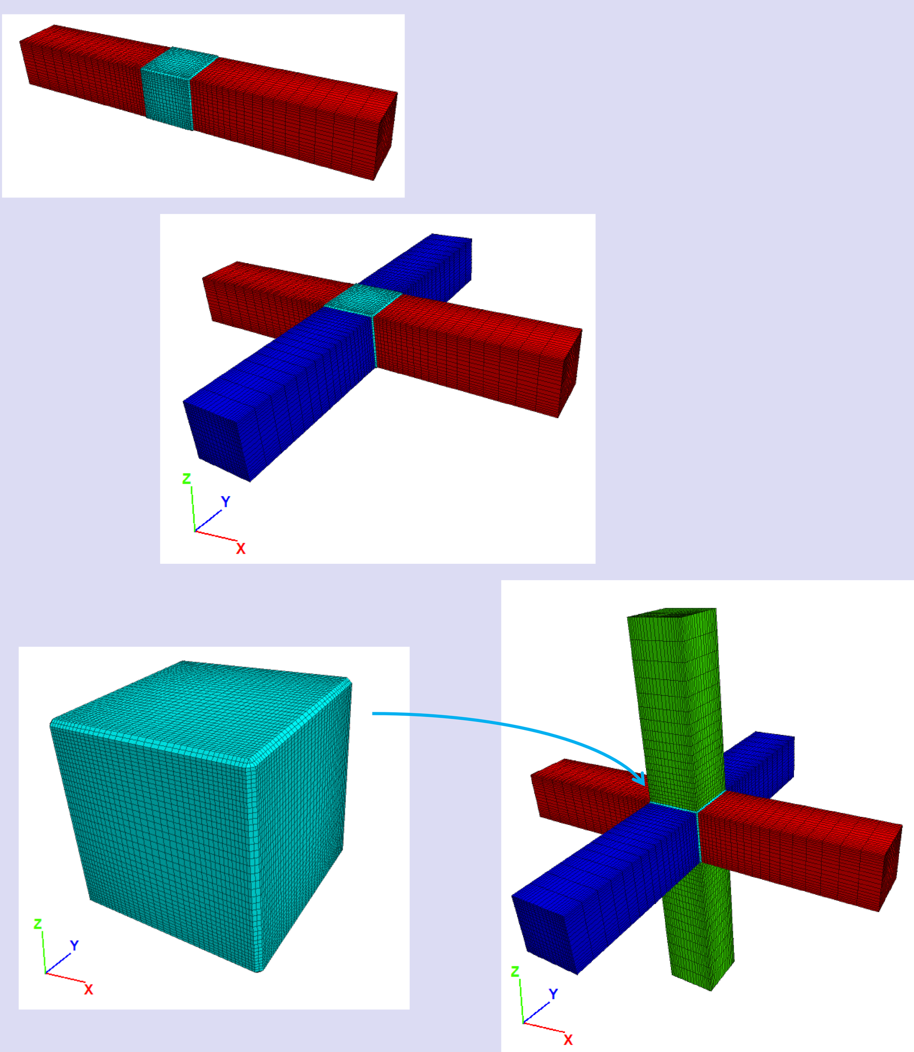

Model Geometry of the cubic rock and the 6 surrounding platens of the polyaxial setup

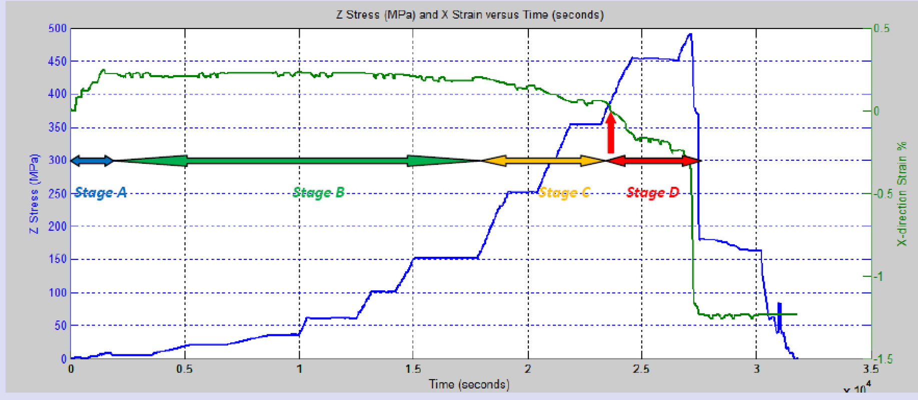

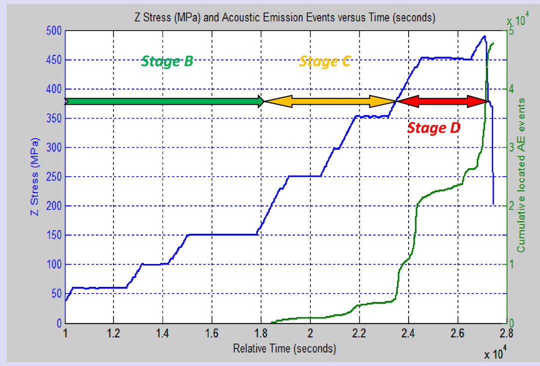

Schematic view of different stages of the Polyaxial test on Fontainbelau Sandstone:
Top: Evolution of main principal stress (blue) and strain in the X-axis (green).
Bottom: : Evolution of main principal stress (blue), cumulative Acoustic Emission Activity (green)

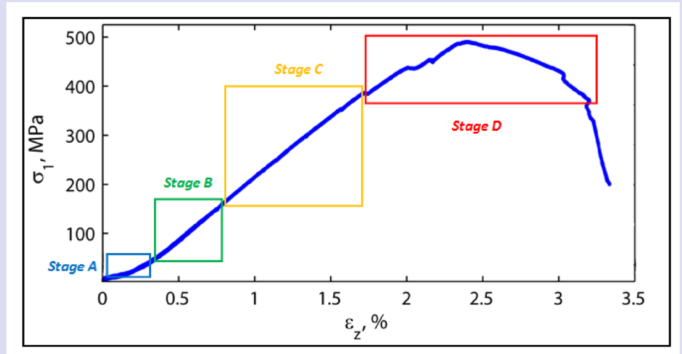

Stress-Strain curve in the main principal stress direction with schematic view of different stages of the experiment.

Table of elastic and plastic model parameters

Rock Elastic Properties		Rock Plastic Properties		Platens' Elastic Properties	
Density (kg/m^3)	2500	Cohesion (Pa)	15e6	Density (kg/m^3)	7500
Bulk Modulus (Pa)	30e9	Friction Angle	40	Bulk Modulus (Pa)	200e9
Shear Modulus (Pa)	20e9	Tension Cutoff (Pa)	5e6	Shear Modulus (Pa)	80e9

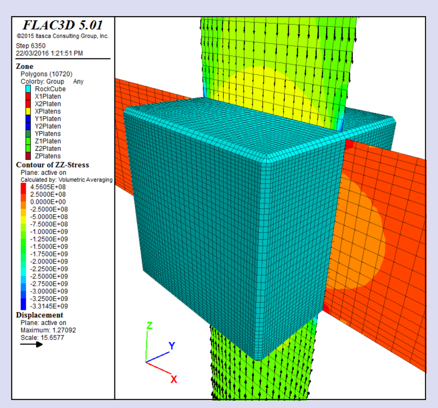

XoZ Cross-sectional plane represented in the following 2D figures along with the XX (left) and ZZ (right) stress distribution

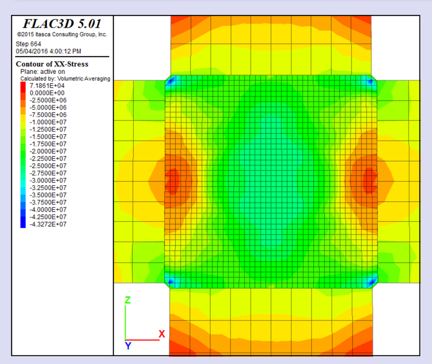

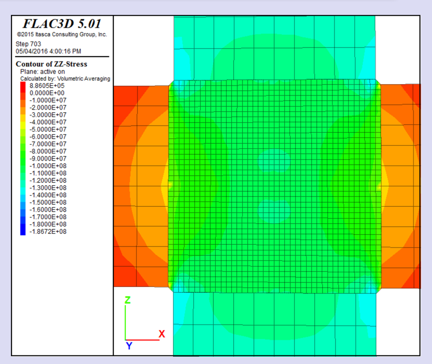

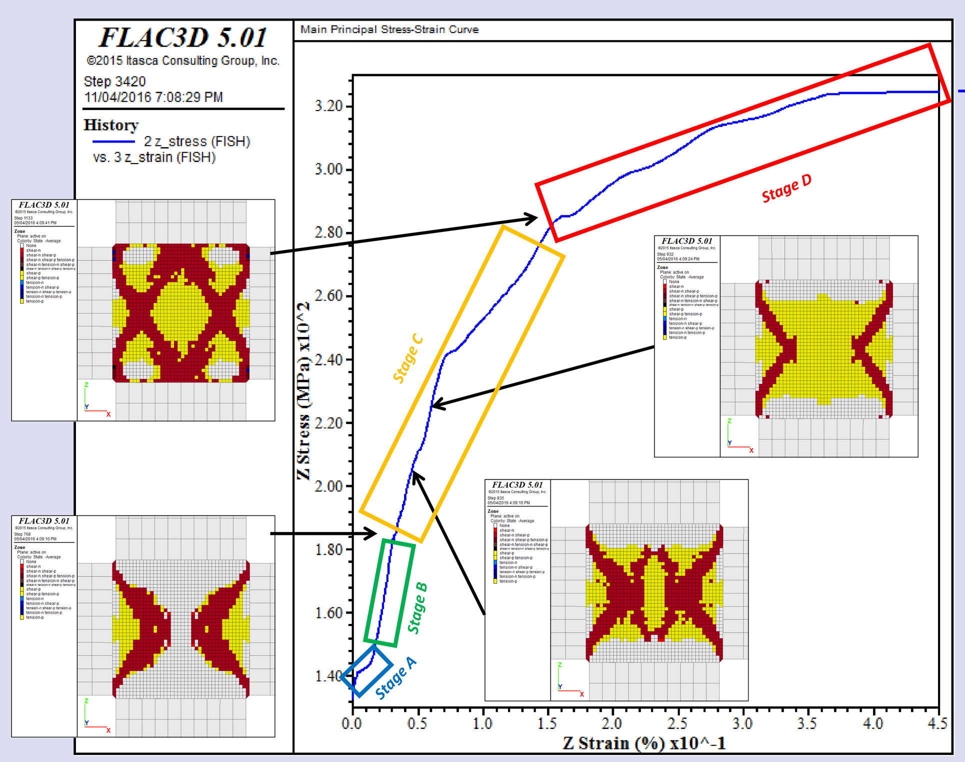

FLAC3D modeling of the failure Process for σ2 = 35 MPa , σ3 = 5 MPa

Fracturing Initiation and propagation process under 28 various Stress Paths while the σ_2 and σ_3 are kept constant and σ_1 is increasing under displacement control with constant rate of 0.0002 (mm/s).

σ2 = 1 MPa σ3 = 1 MPa

σ2 = 5 MPa σ3 = 1 MPa

σ2 = 10 MPa σ3 = 1 MPa

σ2 = 20 MPa σ3 = 1 MPa

σ2 = 35 MPa σ3 = 1 MPa

σ2 = 50 MPa σ3 = 1 MPa

σ2 = 100 MPa σ3 = 1 MPa

σ2 = 5 MPa σ3 = 5 MPa

σ2 = 10 MPa σ3 = 5 MPa

σ2 = 20 MPa σ3 = 5 MPa

σ2 = 35 MPa σ3 = 5 MPa

σ2 = 50 MPa σ3 = 5 MPa

σ2 = 100 MPa σ3 = 5 MPa

σ2 = 10 MPa σ3 = 10 MPa

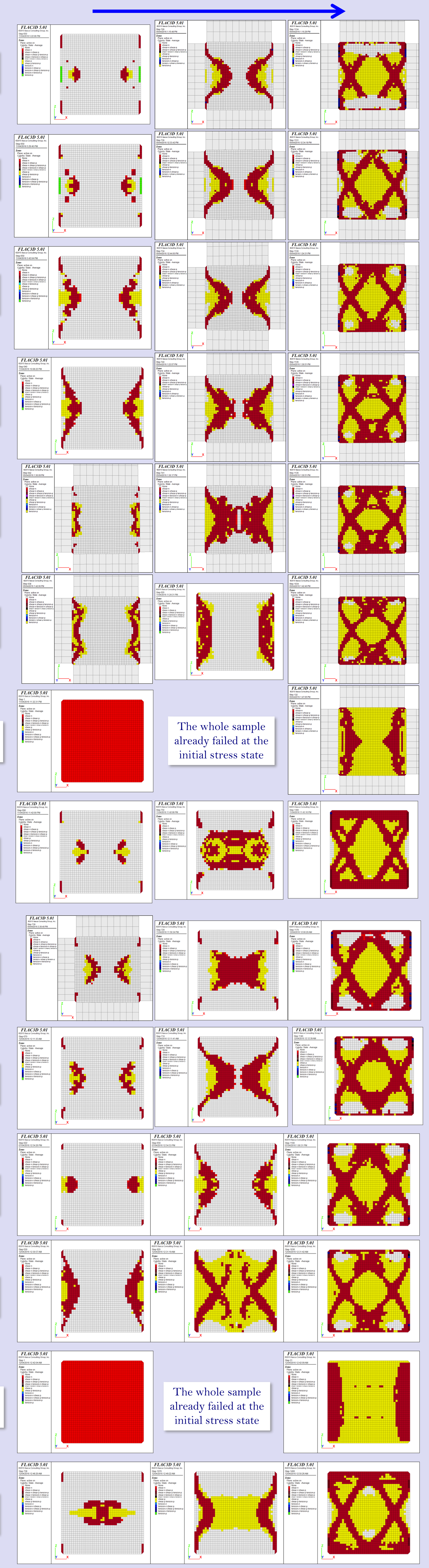

σ2 = 20 MPa σ3 = 10 MPa

σ2 = 35 MPa σ3 = 10 MPa

σ2 = 50 MPa σ3 = 10 MPa

σ2 = 100 MPa σ3 = 10 MPa

σ2 = 20 MPa σ3 = 20 MPa

σ2 = 35 MPa σ3 = 20 MPa

σ2 = 50 MPa σ3 = 20 MPa

σ2 = 100 MPa σ3 = 20 MPa

σ2 = 35 MPa σ3 = 35 MPa

σ2 = 50 MPa σ3 = 35 MPa

σ2 = 100 MPa σ3 = 35 MPa

σ2 = 50 MPa σ3 = 50 MPa

σ2 = 100 MPa σ3 = 50 MPa

σ2 = 100 MPa σ3 = 100 MPa

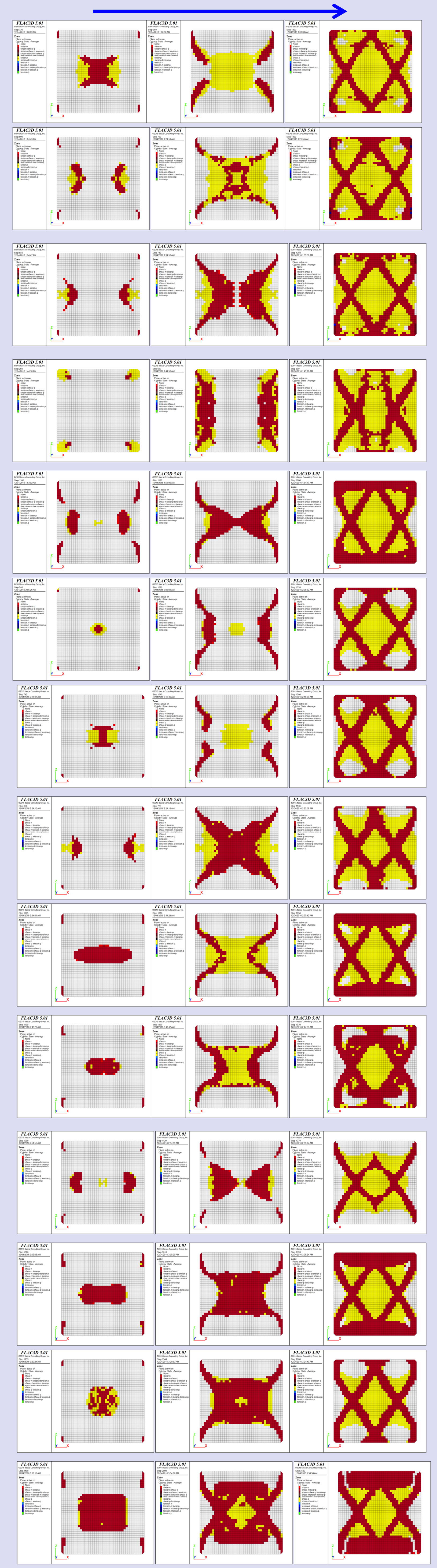

σ_2/σ_3 ratio	σ_2 (MPa): 1	5	10	20	35	50	100
σ_3 (MPa): 1	1	5	10	20	35	50	100
5	×	1	2	4	7	10	20
10	×	×	1	2	3.5	5	10
20	×	×	×	1	1.75	2.5	5
35	×	×	×	×	1	1.43	2.86
50	×	×	×	×	×	1	2
100	×	×	×	×	×	×	1

σ2 / σ3 ratio

	σ_2 (MPa): 1	5	10	20	35	50	100
σ_3 (MPa): 1	57.6°	56.3°	55.9°	55.5°	55.5°	54.8°	NA
5	×	57.6°	57.2°	55.8°	55.5°	57.6°	NA
10	×	×	59.3°	58.8°	57.2°	56.7°	NA
20	×	×	×	59.5°	56.7°	56.7°	57.4°
35	×	×	×	×	56.3°	56.3°	56.1°
50	×	×	×	×	×	57.1°	56.3°
100	×	×	×	×	×	×	54.8°

Failure plane spatial orientation (dip angle)

	σ_2 (MPa): 1	5	10	20	35	50	100
σ_3 (MPa): 1	110	114	119	130	144	155	NA
5	×	114	119	131	144	159	NA
10	×	×	126	145	160	164	NA
20	×	×	×	163	182	194	221
35	×	×	×	×	193	208	252
50	×	×	×	×	×	222	280
100	×	×	×	×	×	×	330

Yield Stress (MPa)

	σ_2 (MPa): 1	5	10	20	35	50	100
σ_3 (MPa): 1	260	268	276	290	315	334	390
5	×	276	286	302	324	345	406
10	×	×	298	316	340	363	424
20	×	×	×	341	369	395	464
35	×	×	×	×	407	440	521
50	×	×	×	×	×	479	579
100	×	×	×	×	×	×	776

Failure Strength or Maximum Stress (MPa)

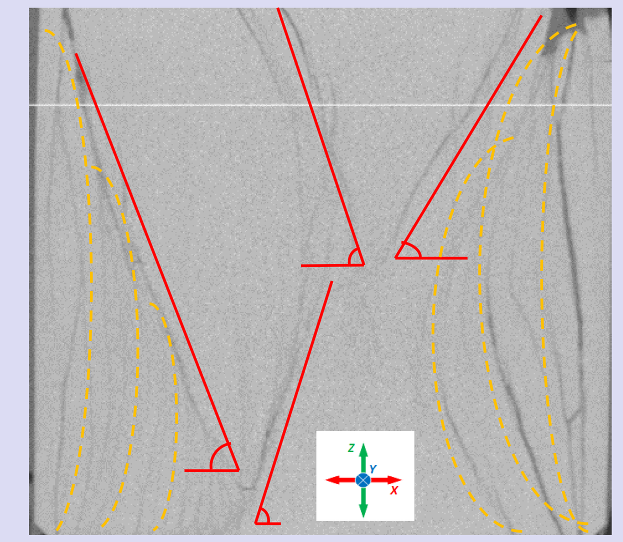

Post mortem cross-sectional CT Scan image of the specimen after the experiment. The dip angles vary between 59° and 65°.

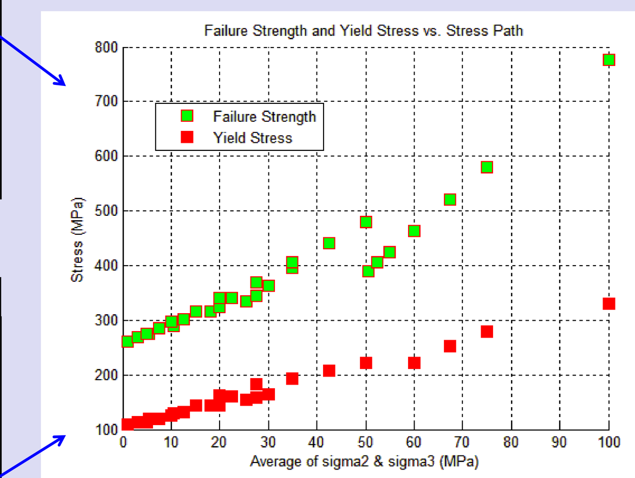

Discussion

This study investigates the effect of stress path on the failure process in the TTT. This is accomplished by applying various constant σ2 and σ3 stresses under load control conditions while the σ1 increased under displacement control condition with a certain displacement rate behind the Z platens in the polyaxial setup. Displacement Rate in the Main Principal Stress (σ1) Direction (Z direction) was 0.0002 (mm/s) with our 80 mm side cube. Different displacement rates definitely create different results. The results were expressed by the yield stress, failure strength and the fracturing angles.

Yielding Stress here is the first stress drop in the stress-strain curve usually when the initial failure in any of the grid nodes occurs. Maximum Strength or Failure Criteria is the point where the stress-strain curve bends down in the numerical simulation of TTT by FLAC3D. That is where the failure plane has already gone through the whole way in the sample along the σ1 direction.

The failure patterns show similar features for similar σ3 / σ2 ratio. The numerical model resembling our laboratory experiment stress path conditions resulted in the failure process which is consistent with the failure pattern in the lab including both curvi-planar fractures and the later through-going fractures. However, the curvi-planar fractures grew on one side of the rock in the experiment because there is always a heterogeneity in reality. Also, the failure strength was higher in the experiment (~500 MPa) compared to the failure strength in the model (~ 325 MPa) and that is because the Mohr-Coulomb failure criteria is too simple for an accurate model of the TTT. However, we just started developing our model and we got perfect results on the fracture geometries out of the networking process between the failed nodes. In the nest steps, we will develop the code based on other failure criteria in FLAC3D as well as 3DEC in order to reproduce the real experimental results more accurately.

Key References

1. Tabari, M. G. (2015). Time-lapse Ultrasonic Imaging of Elastic Anisotropy in Saturated Sandstone under Polyaxial Stress State (Doctoral dissertation, University of Toronto).
2. Itasca (2012). FLAC3D – Three Dimensional Fast Lagrangian Analysis of Continua. Version 5.01. Itasca Consulting Group Inc.